Am J Physiol Cell Physiol 308: C319–C329, 2015.
First published December 4, 2014; doi:10.1152/ajpcell.00253.2014.

Effect of p53 on mitochondrial morphology, import, and assembly in skeletal muscle

Ayesha Saleem,[1,2]* Sobia Iqbal,[1,2]* Yuan Zhang,[1,2] and David A. Hood[1,2]

[1]*School of Kinesiology and Health Science, York University, Toronto, Ontario, Canada; and* [2]*Muscle Health Research Centre, York University, Toronto, Ontario, Canada*

Submitted 17 July 2014; accepted in final form 24 November 2014

Saleem A, Iqbal S, Zhang Y, Hood DA. Effect of p53 on mitochondrial morphology, import, and assembly in skeletal muscle. *Am J Physiol Cell Physiol* 308: C319–C329, 2015. First published December 4, 2014; doi:10.1152/ajpcell.00253.2014.—The purpose of this study was to investigate whether p53 regulates mitochondrial function via changes in mitochondrial protein import, complex IV (COX) assembly, or the expression of key proteins involved in mitochondrial dynamics and degradation. Mitochondria from p53 KO mice displayed ultra-structural alterations and were more punctate in appearance. This was accompanied by protein-specific alterations in fission, fusion, and mitophagy-related proteins. However, matrix-destined protein import into subsarcolemmal or intermyofibrillar mitochondria was unaffected in the absence of p53, despite mitochondrial subfraction-specific reductions in Tom20, Tim23, mtHsp70, and mtHsp60 in the knockout (KO) mitochondria. Complex IV activity in isolated mitochondria was also unchanged in KO mice, but two-dimensional blue native-PAGE revealed a reduction in the assembly of complex IV within the IMF fractions from KO mice in tandem with lower levels of the assembly protein Surf1. This observed defect in complex IV assembly may facilitate the previously documented impairment in mitochondrial function in p53 KO mice. We suspect that these morphological and functional impairments in mitochondria drive a decreased reliance on mitochondrial respiration as a means of energy production in skeletal muscle in the absence of p53.

protein import machinery; fission/fusion; mitophagy; cytochrome *c* oxidase assembly

p53, THE "GUARDIAN OF THE GENOME," monitors and maintains genomic stability. Mutations in, or loss of, p53 results in detrimental consequences, including an increased susceptibility to cancer (20). In response to cellular stress, such as oncogenic activation and DNA damage, p53 responds by coordinating mechanisms to prevent and/or repair genomic damage or by targeting the removal of dysfunctional components. Consistent with this, p53 is capable of upregulating and/or suppressing apoptosis and autophagy to enhance cell survival. While apoptosis refers to cell death, autophagy involves the sequestering of cytoplasmic material, its encapsulation, and eventual digestion through delivery to the lysosome in response to stressful conditions and as a means of removal of damaged or superfluous organelles and proteins (12).

During general autophagy induction, the proautophagy proteins Beclin1, ULK1, and ATG7 initiate the formation of the autophagosome. Selective removal of dysfunctional mitochondria (mitophagy) is induced as a result of elevated mitochondrial reactive oxygen species production (43), as well as the dissipation of the mitochondrial membrane potential (36, 50). During this process, the cytosolic E3 ubiquitin ligase Parkin is recruited to dysfunctional organelles with reduced membrane potential in a PINK1-dependent manner, thereby promoting mitophagy (30). p62 binds to the ubiquitinated mitochondria and acts as an adaptor for the organelles to be recognized by the autophagic marker LC3 (3, 32, 33), and it is degraded in the process as well (3, 19). Subsequently, LC3II, a processed form of LC3, is localized in the membranes participating in the mitophagy process, and its content reflects the number of autophagosomes present in the tissue (18). Upon encapsulation of the dysfunctional mitochondria, the autophagosome delivers this material to the lysosome for degradation, where lysosomal proteinases such as cathepsin D participate in its degradation (51).

Recent studies have examined the effects of inactivating p53 and found that the loss of p53 induces autophagy within human cells (48, 49). Interestingly, other work suggests that the subcellular compartmentalization of p53 ultimately determines its effect on autophagy within the cell. For example, cytoplasmic p53 inhibits autophagy through a transcription-independent effect, whereas the nuclear localization of p53 induces the activation of autophagy genes (15, 29, 49). To determine how the autophagy and mitophagy processes were affected by the ablation of p53, we examined key proteins involved in these pathways, as well as the localization of important autophagy markers.

In addition to this divergent effect on autophagy, the subcellular localization of p53 also dictates how this protein affects mitochondrial function (1). p53 plays a vital role in maintaining optimal mitochondrial content and function, and the absence of this protein is detrimental to endurance capacity (38, 39). The tumor suppressor protein p53 was first identified to affect oxidative capacity via its ability to transcriptionally regulate synthesis of cytochrome *c* oxidase 2 (SCO2), an important accessory factor in mitochondrial complex IV assembly (25). Subsequently, we and others demonstrated lower complex IV activity in whole muscle homogenates, along with several impaired indexes of mitochondrial function evident in the p53 KO mice (35, 38). Like many other complexes of the electron transport chain (ETC) in the mitochondria, cytochrome *c* oxidase (COX) is made up of both mtDNA- and nuclear DNA-encoded proteins, rendering mitochondrial protein import as an important determining factor in the biogenesis of the complex.

Mitochondrially destined proteins are synthesized by ribosomes in the cytosol and are guided to the mitochondrion by cytosolic chaperones such as heat shock protein 70 (Hsp70), Hsp90, and mitochondrial import stimulating factor (MSF; 27, 28, 57). These chaperones deliver the proteins directly to the translocase of the outer mitochondrial membrane (TOM) com-

* A. Saleem and S. Iqbal contributed equally to this work.

Address for reprint requests and other correspondence: D. A. Hood, School of Kinesiology and Health Science, York Univ., Toronto, Ontario M3J 1P3, Canada (e-mail: dhood@yorku.ca).

plex where the import process begins. Tom20 is one of the receptor proteins on the TOM complex that recognizes and binds to cytosolic preproteins (5, 31, 37). Once through the TOM complex, the precursor proteins can be directed towards different pathways depending on whether the protein is targeted to the outer mitochondrial membrane, inner membrane, intermembrane space, or the matrix (44). Precursor proteins destined for the matrix are imported by the translocase of the inner membrane (TIM) complex, through the channel-forming Tim23 protein (5, 31, 56) with the assistance of the presequence translocase-associated motor (PAM). The core of PAM is composed of mitochondrial heat shock protein 70 (mtHsp70) that actively pulls the unfolded preprotein into the matrix in an ATP- and $\Delta\Psi$-dependent manner (5, 31). The precursor proteins undergo processing and are folded into their final configurations with the assistance of mtHsp60 and chaperonin 10 (cpn10) (14).

Furthermore, to maintain the integrity of mitochondria, cycles of fission and fusion events occur, whereby the selective removal and inability to refuse damaged or dysfunctional organelles are critical. The fusion process involves the mixing of mitochondrial material through the use of the remodeling proteins Mfn2 and Opa1 (6, 26). Fission events divide the damaged organelle into smaller, fragmented components via Drp1 and Fis1 proteins, suitable for removal by the autophagosome through a process known as mitophagy (50). Parkin is an important component of the mitophagy process, and it also plays a critical role in modulating the morphology of mitochondria, such that inhibition of mitochondrial fission has been demonstrated to reduce Parkin-mediated mitophagy (47). Therefore, the PINK1/Parkin pathway is thought to be the intermediate step between mitochondrial remodeling and mitophagy.

Thus the purpose of this study was to investigate the role of p53 in regulating protein import and complex assembly within skeletal muscle, using p53 knockout mice. We also sought to determine the effects of p53 ablation on mitochondrial autophagy, fission/fustion, and morphology, since compromised levels of p53 have previously been shown to result in an irregular mitochondrial architecture (38). Our results will help elucidate the role of p53 in mitophagy, import signaling, and organelle morphology in skeletal muscle.

MATERIALS AND METHODS

Animal breeding. Transgenic p53 mice (10) were obtained from Taconic Laboratories. Heterozygous p53 mice were bred to obtain wild-type (WT) and p53 homozygous knockout (KO) mice. Each progeny of the breeding pair was genotyped as follows. An ear clipping obtained from each animal was used for a crude DNA extraction. Extracted DNA was added to a PCR tube containing DNA Taq Polymerase (Sigma Jumpstart REDtaq Ready Mix PCR Reaction Mix) and forward and reverse primers for the WT p53 gene or the KO p53 gene. Differences in the genome were detected using PCR amplification. The reaction products were separated on a 2% agarose gel at 90 volts for 2–2.5 h and visualized with the use of ethidium bromide. The use of animals was approved by the York University Animal Care Committee.

Experimental design. At ~3 mo of age, p53 KO and their WT littermates (n = 9/group) were cervically dislocated, and the quadriceps femoris, and gastrocnemius muscle groups were excised and placed in ice-cold buffer for cytosolic and mitochondrial fractionation. The protein content of cytosolic and mitochondrial extracts was determined using the Bradford method (4).

Mitochondrial and cytosolic fractionation. Freshly isolated muscle tissue (quadriceps femoris and gastrocnemius) was minced, homogenized, and subjected to differential centrifugation to isolate the subsarcolemmal (SS) and intermyofibrillar (IMF) mitochondrial subfractions, as described previously (7, 23, 46). Briefly, muscle was excised and minced thoroughly after trimming excess fat and connective tissue. Minced tissue samples were diluted 10-fold with *buffer 1* (l00 mM KCl, 5 mM $MgSO_4$, 5 mM EDTA, 50 mM Tris·HCl pH 7.4, and 1 mM ATP), homogenized for 10 s with an Ultra-Turrax polytron at 50% power, and then spun at 800 *g* for 10 min. The supernate was filtered through a cheesecloth, centrifuged at 9,000 *g* (10 min) to obtain SS mitochondria. The pellet from the first 800 *g* spin was resuspended in *buffer 1*, centrifuged at 9,000 *g* (10 min), resuspended by hand using a loose-fitting Teflon-coated pestle, rehomogenized with the polytron, and recentrifuged at 800 *g* (10 min). Subsequently, the pellet was resuspended in a 10-fold dilution with *buffer 2* [100 mM KCl, 5 mM $MgSO_4$, 5 mM ethyl glycol-bis(β-aminoethyl ether)-*N*,*N*,*N*′,*N*′-tetraacetic acid, 1 mM ATP, and 50 mM Tris·HCl pH 7.4]. Samples were then incubated for 5 min with the protease nagarse (2.5 mg nagarse/g tissue), and the reaction was stopped afterwards with the addition of 20 ml of *buffer 2*, followed by centrifugation at 5,000 *g* for 5 min. The pellet was discarded and the supernate was taken and spun at 9,000 *g* (10 min) to isolate the IMF subfraction. SS and IMF mitochondrial pellets were suspended in resuspension medium (100 mM KCl, 10 mM MOPS, and 0.2% BSA). All steps were carried out at 4°C. After the isolation procedure, SS and IMF mitochondria were used for analyses of mitochondrial protein import, two-dimensional blue native-PAGE (2D BN-PAGE), cytochrome *c* oxidase enzyme activity and immunoblotting. Cytosolic fractions were prepared from freshly isolated skeletal muscle using a commercially available extraction kit (Pierce NE-PER, Rockford, IL). Briefly, 50–75 mg of skeletal muscle were minced and homogenized in CER-I buffer containing protease inhibitor cocktail Complete, EDTA-free (Roche Applied Sciences, Manheim, Germany). After a series of wash steps, the cytosolic fraction was obtained as the supernate following centrifugation at 100,000 *g* at 4°C for 60 min.

Transmission electron microscopy. Samples from the gastrocnemius muscles were prepared and analyzed as previously described (13). Briefly, muscle samples were incubated on ice in 3% glutaraldehyde buffered with 0.1 M sodium cacodylate for 1 h. Muscle sections were then washed 3 × 15-min with 0.1 M sodium cacodylate, followed by incubation in 1% osmium tetroxide in 0.1 M sodium cacodylate at room temperature. After sections were fixed for proteins and lipids, samples were subjected to gradient dehydration of 30, 50, 80, and 100% anhydrous ethanol. Next, sections were embedded in a 1:1 solution of fresh Spurr's embedding resin and anhydrous ethanol overnight. Groups of muscle fibers were then dissected from the sections and embedded in fresh Spurr's embedding resin and incubated at 60°C for 48 h. Ultrathin sections (60 nm) were cut, placed on copper grids, and poststained with uranyl acetate and lead citrate. Electron micrographs were imaged on a Philips EM201 electron microscope (FEI, Hillsboro, OR).

The area occupied by IMF mitochondria within 4 μm^2 and the maximal SS depth were assessed based on electron micrograph images taken at ×20,000–45,000 magnifications. Calibrations were performed before measurements to account for the magnification of the images. To determine the maximal depth of SS mitochondria, a line was drawn from the outer edge of the most peripheral mitochondria to the edge of the myofibril. The line was placed perpendicular to the myofibril. The maximal distance between the mitochondria and myofibril was chosen in each case. When assessing the area occupied by IMF mitochondria, 4-μm^2 squares were randomly placed throughout the image in a nonoverlapping fashion to ensure that the organelles were not repeatedly counted.

COX enzyme activity. COX activity was measured as previously detailed (8). Briefly, mitochondrial extracts were added to a test solution containing fully reduced cytochrome *c*. Enzyme activity was determined as the maximal rate of oxidation of fully reduced cytochrome *c* measured by the change in absorbance at 550 nm in a Synergy HT microplate reader at 30°C.

DNA isolation and in vitro transcription. The full-length cDNA clone for ornithine transcarbamylase (OCT), a matrix-bound mitochondrial protein, was a generous gift from Dr. Gordon Shore (McGill University, Montreal, Canada). The vector containing the OCT cDNA was linearized using *Sac* I at 37°C for 2 h. Plasmid DNA was subsequently phenol extracted and ethanol precipitated overnight at −80°C. The DNA was diluted to a concentration of 0.8 μg/μl and was transcribed at 40°C for 90 min using SP6 RNA polymerase. The resulting mRNA pellet was resuspended to a final concentration of 2.8 μg/μl, and aliquots were stored at −80C for use in import assays.

In vitro translation and import. The pOCT mRNA underwent in vitro translation in the presence of [^{35}S]methionine within a rabbit reticulocyte lysate system. Briefly, isolated SS and IMF mitochondria were allowed to equilibrate by preincubation for 10 min at 30°C before the import assay. Translation mix (12 μl per 50 μg of mitochondrial protein) was added to the mitochondria, and the import incubation was allowed to proceed at 30°C for 20 min. After 20 min, import was stopped by applying the mitochondrial translation mix to an ice-cold sucrose cushion (in mM: 600 sucrose, 100 KCl, 20 HEPES, and 2 $MgCl_2$). Mitochondria were pelleted by centrifugation for 15 min at 16,000 *g* (4°C) and resuspended in 20 μl of ice-cold breaking buffer (600 mM sorbitol and 20 mM HEPES pH 7.4). The samples were denatured for 5 min and electrophoresed through a 12% SDS-polyacrylamide gel. Gels were processed and dried with a vacuum gel dryer. Radiolabeled precursor and mature proteins were detected using phosphorimaging (Pharos FX; Bio-Rad) and quantified with electronic autoradiography (Quantity One; Bio-Rad, Hercules, CA). The percentage of protein import was calculated based on the ratio of the intensity of the mature OCT and total OCT (sum of mature and precursor bands). A translation lane mixture was run on each gel as a control for the in vitro translation and import reaction.

2D BN-PAGE. Separation of electron transport complexes was performed using BN-PAGE according to the protocol described by Schagger and colleagues (41, 42). Mitochondrial fractions (200 μg) were solubilized with η-dodecyl β-D maltoside in a buffer composed of 750 mM ε-amino-η-caproic acid, 50 mM Bis-Tris pH 7.0, at 4°C. Following solubilization, samples were centrifuged for 25 min at 100,000 *g* at 4°C. Coomassie G-250 was added to the resulting supernatants using a detergent-to-dye ratio of 4:1 (wt/wt). The supernatants were applied on a 5–13% gradient BN PAGE gel and electrophoresed overnight for 16 h at 4°C and 23 V. To perform 2D BN-PAGE, strips from the first dimension were cut, rotated 90°, and subjected to further separation in the second dimension on a 12% denaturing SDS gel. After electrophoresis, proteins were electroblotted onto PVDF membranes and subsequently probed with COX-I (complex IV) antibody as described below.

Immunoblotting. Isolated mitochondrial and cytosolic protein extracts were separated using 10–15% SDS-PAGE and subsequently transferred onto nitrocellulose membranes. Membranes were then blocked (1 or 1.5 h) with a 5% skim milk in 1× TBS-Tween 20 solution (Tris-buffered saline-Tween 20: 25 mM Tris·HCl pH 7.5, 1 mM NaCl, and 0.1% Tween 20) at room temperature, followed by incubation in blocking solution with antibodies directed towards Fis1 (1:500; Alexis Biochemical); Drp1 (1:500) and Opa1 (1:500; BD Transduction Laboratories); Mfn2 (1:250; Sigma), porin/VDAC (1:3,000; Abcam); ULK1 (1:500; Sigma); Parkin (1:500; Santa Cruz), p62 (1:5,000; Sigma); LC3II (1:500; Cell Signaling); NIX (1:200; Abcam); Tom20 (Santa Cruz Biotechnology), Tim23 (BD Biosciences); mtHsp70, mtHsp60, and cpn10 (Assay Designs); hsp70 and hsp90 (Stressgen Bioreagent); MSF-L (a kind gift from Dr. K. Mihara, Kyushu University); Surfeit locus protein 1 (Surf1; a kind gift of Dr. E. Shoubrdige, McGill University); mitochondrial ETC cocktail and COX-I (Mitosciences); and aciculin overnight at 4°C. Subsequently, membranes were washed three times for 5 min with TBS-Tween 20, followed by incubation at room temperature (1 h) with the appropriate secondary antibody conjugated to horseradish peroxidase, and washed again three times for 5 min each with TBS-Tween20. Membranes were developed using Western Blot Luminol Reagent (Santa Cruz Biotechnology), and films were subsequently scanned and quantification via densitometric analysis for the intensity of signals with SigmaScanPro software (version 5; Jandel Scientific, San Rafael, CA).

Statistical analysis. Data were analyzed using Graph Pad 4.0 software and values are reported as means ± SE unless otherwise indicated. Mitochondrial protein import and COX activity were analyzed using a two-way ANOVA and Bonferroni posttests. All other data were analyzed using Student's *t*-test. Significance levels were set at $P < 0.05$.

RESULTS

Ablation of p53 causes aberrant mitochondrial structures. To examine the effects of p53 on the morphology of mitochondria, we compared electron microscopy images of the gastrocnemius muscle from p53 KO mice with those of their age-matched WT counterparts. Transmission electron microscopy revealed disruptions in mitochondrial content and structure in both SS and IMF subfractions in the absence of p53. We observed that the loss of p53 reduced SS mitochondrial content, as evident by the 61% reduction in the thickness of the SS mitochondrial layer ($P < 0.05$; Fig. 1*D*). The lower mitochondrial content correlates with the reduced levels of whole muscle COX activity in p53 KO mice, as we previously demonstrated (38). Furthermore, mitochondrial cristae disruptions increased drastically upon ablation of p53 (Fig. 1*B*, *bottom*). The shape of the cristae appeared disorganized and an accumulation of unidentified cellular material often localized within the organelles. The disorganization of mitochondrial cristae structure was accompanied by the dismantling of IMF mitochondria into smaller fragments. To avoid quantification errors that may have occurred from individual assessments, we measured the total area occupied by IMF mitochondria. p53 KO animals displayed a 70% reduction in the area occupied by IMF mitochondria compared with their WT counterparts ($P < 0.05$; Fig. 1*C*).

Expression of mitochondrial morphology proteins. To understand the molecular basis of the observed fragmentation, we assessed the expression levels of the proteins governing mitochondrial morphology. We measured the protein expression of Fis1, Drp1, Opa1, and Mfn2 mitochondrial morphology machinery components (Fig. 2*A*). Within isolated SS mitochondria, the expression of the fusion proteins (Opa1 and Mfn2) was not altered by the absence of p53 (Fig. 2*B*). However, the lack of p53 resulted in a divergent expression patterns for the fission proteins, with cytosolic Drp1 content reduced by 44% ($P < 0.05$) and Fis1 expression enhanced by 80% ($P < 0.05$). These results illustrate that p53 has a differential effect on the expression of organelle fission proteins.

Expression and localization of autophagy and mitophagy proteins in the absence of p53. While we have not measured the rates of autophagy and mitophagy in these animals, we performed a preliminary examination of the expression of key proteins involved in autophagy (ULK1; Fig. 3, *C* and *D*) and mitochondrial cargo selection, Parkin, p62, mature LC3

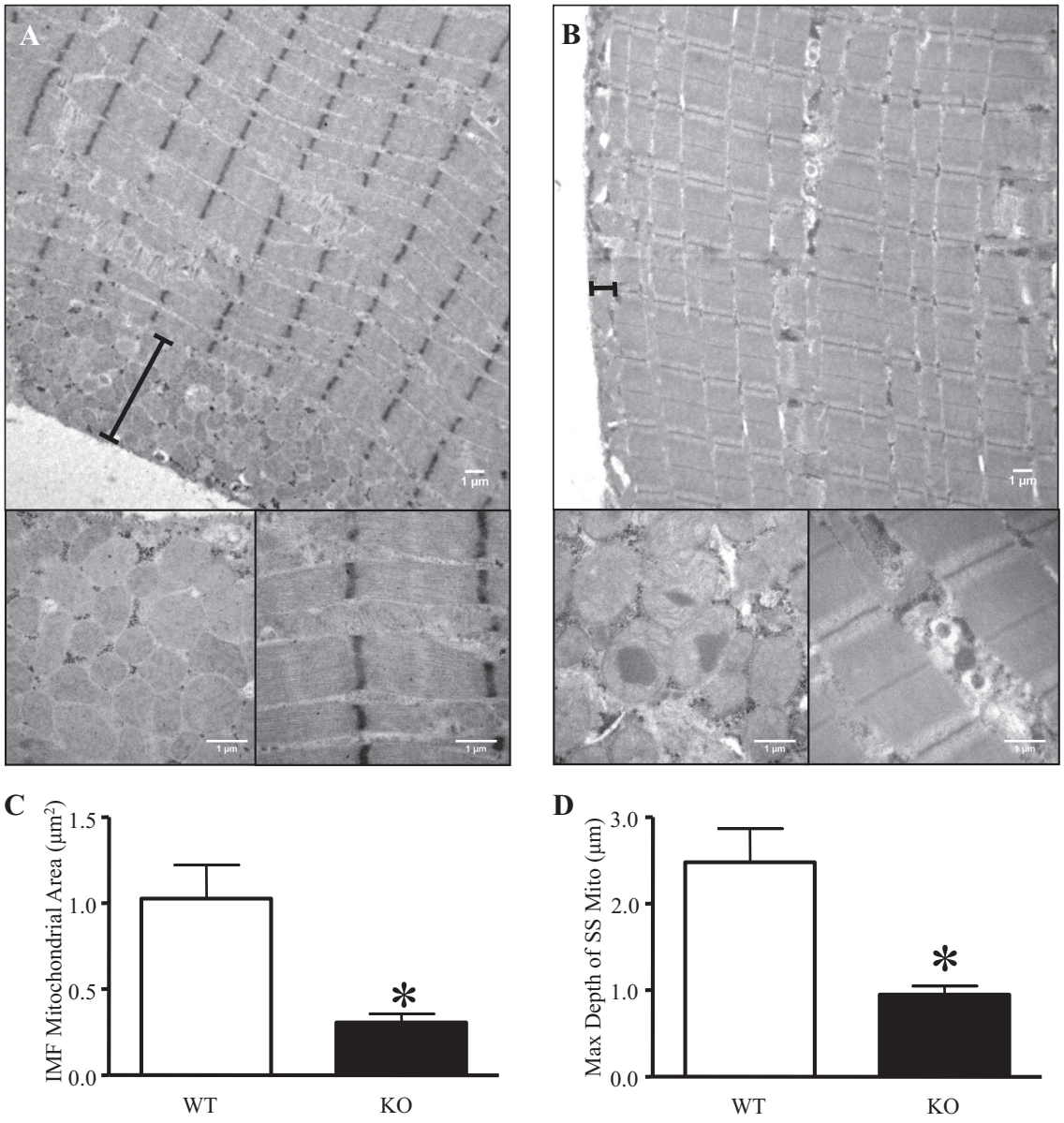

Fig. 1. Electron micrographs of skeletal muscle from wild-type (WT; *A*) and p53 knockout (p53 KO; *B*) mice. Morphological alterations in mitochondria are visualized by the representative images taken at a magnification of ×7,000 and ×30,000 (*bottom*). Images taken at ×30,0000 of subsarcolemmal (SS) mitochondria are shown at *bottom left* and intermyofibrillar (IMF) mitochondria appear at *bottom right*. Quantification of the total area occupied by IMF mitochondria in 4 μm^2 area (*C*) and the maximal depth of the SS layer (*D*); $n = 4$–7; $^*P < 0.05$ vs. WT.

(LC3II), and NIX (Fig. 3, *A* and *B*). Within isolated cytosolic fractions, the expression of ULK1 was significantly upregulated by 5.8-fold when p53 was absent ($P < 0.05$; Fig. 3, *C* and *D*). Thus this suggests that the basal levels of p53 likely function to suppress the level of ULK1 during control conditions. Our results demonstrated an 80% downregulation of Parkin within cytosolic fractions, in addition to a 70% reduction in the association of Parkin with SS mitochondria in the absence of p53 ($P < 0.05$; Fig. 3*B*). Similarly, a significant 60% reduction in mitochondrial p62 levels was observed. Interestingly, mitochondrial LC3II localization was upregulated by 64% while a 46% reduction was observed in cytosolic fractions. NIX expression was unaltered in mitochondria from p53 KO animals vs. WT counterparts.

Absence of p53 reduces the expression of several mitochondrial protein import machinery components. Tom20, Tim23, mtHsp70, mtHsp60, and cpn10 are intimately associated with the import and subsequent processing of matrix-destined proteins. Expression of these factors was determined in isolated SS and IMF mitochondrial fractions (Fig. 4, *A* and *B*). In the SS mitochondria, lack of p53 induced a significant reduction in Tom20 (39%), Tim23 (36%), mtHsp70 (56%), and mHsp60 (32%) content, whereas cpn10 expression remained unchanged (Fig. 4*B*). We also observed a significant decrease in the protein levels of Tim23, mtHsp70, and mtHsp60 by ~71, ~56, and ~45%, respectively, in the IMF fractions isolated from p53 KO mice compared with their WT counterparts (Fig. 4*B*). Cpn10

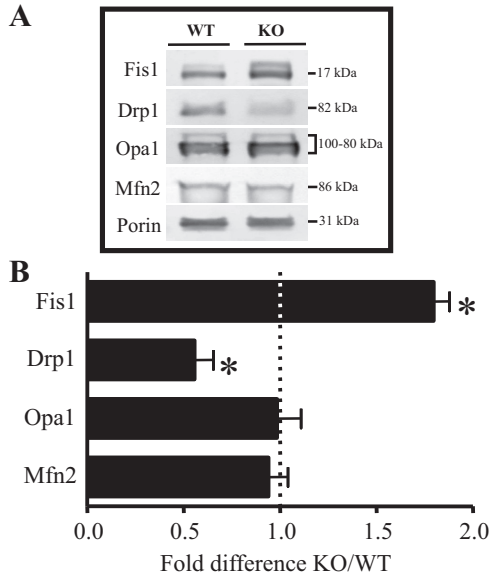

Fig. 2. Mitochondria morphology protein expression in WT and KO muscle. Representative images of Fis1, Drp1, Opa1, Mfn2 protein content (*A*), and graphical quantification (*B*) expressed as fold over WT in SS mitochondrial or cytosolic fractions. Fis1, Opa1, and Mfn2 were determined using SS mitochondrial fractions, whereas Drp1 was assessed in cytosolic fractions. Values are expressed as fold changes (KO/WT) ± SE; $n = 4$; $^*P < 0.05$ vs. WT.

and Tom20 expression were not altered in the IMF mitochondrial pool in p53 KO mice.

Expression of cytosolic chaperones involved in mitochondrial protein import remains unchanged in p53 KO animals. Cytosolic chaperones are known to affect the import of mitochondrial proteins with an NH_2-terminal presequence or internal localization signal. We investigated the expression of Hsp70, Hsp90, and MSF-L in cytosol isolated from p53 WT and KO mice. There was no alteration in the expression of the cytosolic chaperones in p53 KO muscle compared with WT counterparts (Fig. 4*C*).

Import of matrix-destined preproteins into SS and IMF mitochondria is not impaired in p53 KO mice. The import of the matrix-destined precursor protein pOCT into isolated SS and IMF mitochondria is illustrated as a representative autoradiogram with its quantification below (Fig. 5, *A* and *B*). The amount of percent OCT protein import was not significantly altered between SS or IMF mitochondria from p53 KO, compared with WT mice (Fig. 5, *A* and *B*). As has been shown previously (46), the overall level of pOCT import into SS mitochondrial subfraction was lower than that observed in the IMF mitochondria.

Mitochondrial COX activity and expression of ETC machinery components were unaffected in muscle in the absence of p53. Using isolated SS and IMF mitochondria from p53 WT and KO mice, we measured no change in the rate of COX activity (Fig. 6*A*). In addition, the expression of components of the ETC machinery such as complex V ATP synthase subunit α (V), complex III subunit core 2 (III), complex IV subunit I (IV), complex II subunit 30 kDa (II), and complex I subunit NADH-ubiquinone oxidoreductase 1β subcomplex (I) did not differ between the two genotypes in either mitochondrial subfractions (Fig. 6, *B* and *C*).

Impaired assembly of the COX complex in IMF mitochondria derived from p53 KO mice. We used a 2D BN-PAGE technique to specifically analyze the assembly of complex IV in SS (Fig. 7*B*) and IMF mitochondria (Fig. 7*D*) from p53 WT and KO mice. While assembly and synthesis of mature complex IV (S4) was not altered in the SS fraction (Fig. 7*B*), it was decreased by 39% in the IMF mitochondria ($P < 0.05$; Fig. 7*D*). This was

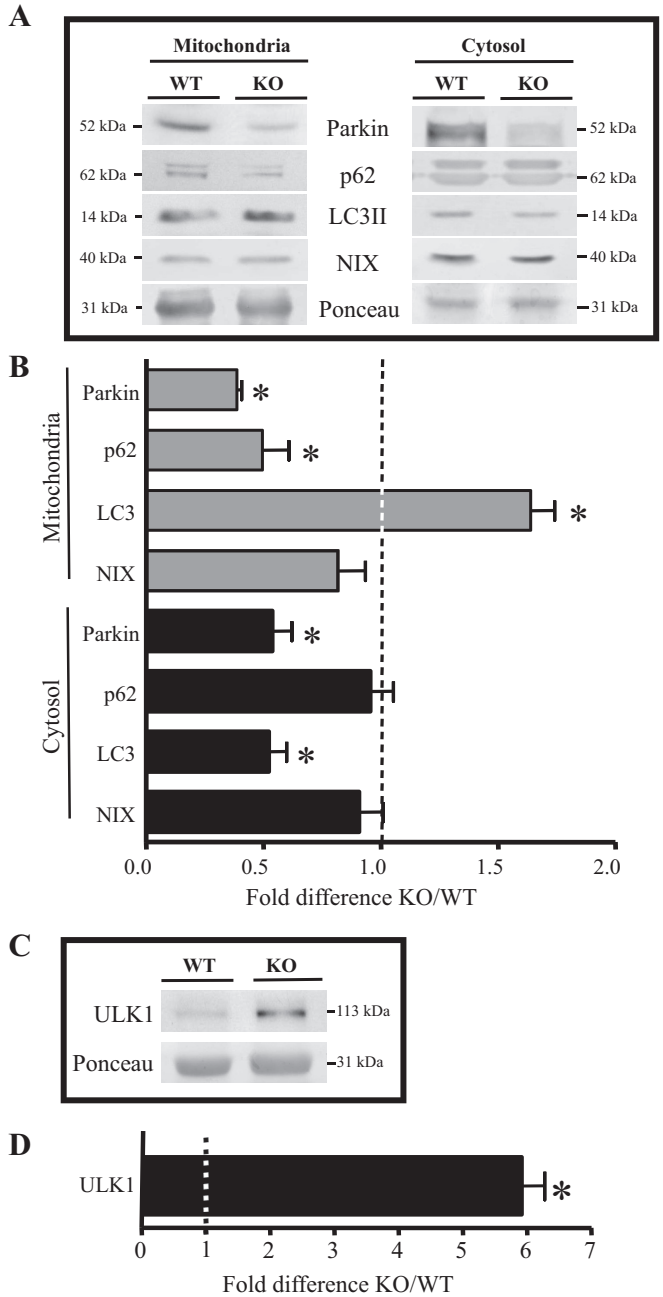

Fig. 3. Effects of p53 depletion on autophagy and mitophagy markers. *A*: Parkin, p62, LC3II, and NIX were assessed by immunoblotting from SS mitochondrial and cytosolic subfractions. Samples were corrected for loading using the Ponceau and voltage-dependent anion channel (VDAC) for cytosolic and SS mitochondrial fractions, respectively. *B*: graphical quantification of each indicated protein is depicted. Representative Western blot of ULK1 from cytosolic fractions (*C*) and graphical quantification are depicted (*D*). Values are expressed as fold changes (KO/WT) ± SE; $n = 4$; $^*P < 0.05$ vs. WT.

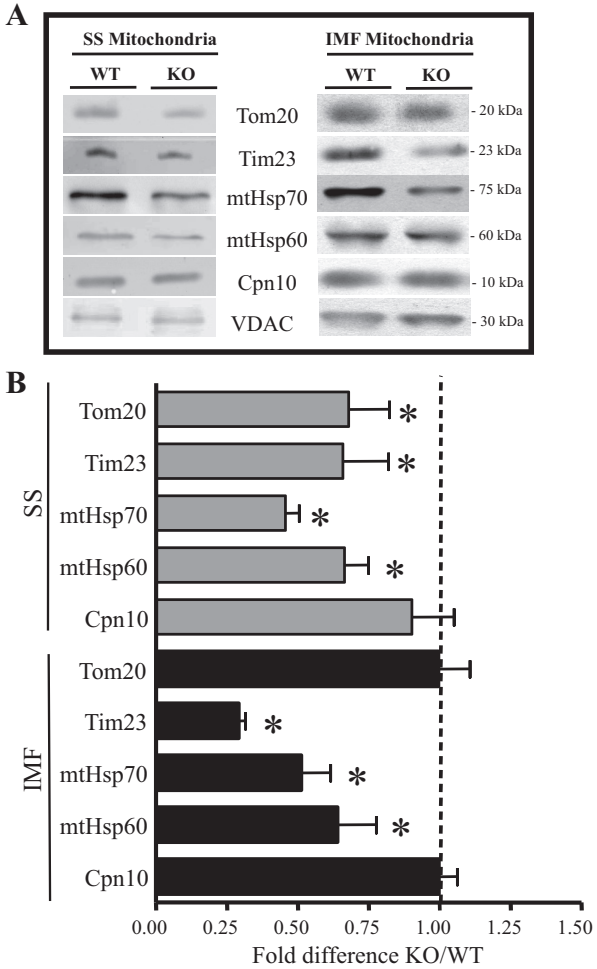

Fig. 4. Effect of p53 on expression of protein import machinery (PIM) components in SS and IMF mitochondria. *A*: representative Western blots of Tom20, Tim23, mtHsp70, mtHsp60, and cpn10 in SS and IMF mitochondria isolated from muscle of p53 WT and KO mice, with the respective *B*: graphical representation. VDAC was unchanged between the two genotypes and was used as a loading control. Values are expressed as fold changes (KO/WT) ± SE; $n = 4–9$; $^*P < 0.05$ vs. WT. *C*: representative Western blots of the cytosolic chaperones heat shock proteins 70 and 90 (Hsp70 and Hsp90) and mitochondrial import stimulating factor (MSF). Aciculin was used as a loading control and did not change between the conditions; $n = 3–6$.

accompanied by a significant 41% decrease in the expression of Surf1 (Fig. 7*C*), an accessory assembly factor that facilitates the assembly of COX in mitochondria. Surf1 expression was not different between the two genotypes in SS mitochondria (Fig. 7*A*).

DISCUSSION

p53 activates numerous metabolic pathways, including oxidative phosphorylation, mitochondrial genomic integrity, fatty acid oxidation, insulin sensitivity, nucleotide biosynthesis, antioxidant responses, and autophagy (24). The coordination of these pathways through p53 can help the cell respond to stressful challenges such as oncogenic activation or DNA damage. By activating or inhibiting cellular pathways, p53 can effectively minimize the accumulation of damaged cellular components, thereby conferring protection from cell death. Interestingly, the diverse effects of p53 on mitochondrial function and oxidative capacity have only begun to be investigated in skeletal muscle. We have previously shown that the removal of p53 compromises not only the activity and content of mitochondria but also the architecture of these organelles (38). To understand some of the underlying mechanisms involved, our study investigated the effect of p53 on mitochondrial protein import and assembly, autophagy protein expression, and mitophagy signaling in p53-deficient muscle under basal, nonstressful conditions.

Mitochondrial synthesis is a highly regulated process that involves the coordination of both the nuclear and the mitochondrial genomes. However, the vast majority (>99%) of mitochondrial proteins are imported into the mitochondria, rendering this process crucial for the synthesis and function of the organelle. Rates of mitochondrial protein import can be regulated by alterations in *1*) mitochondrial respiration, *2*) expression of protein import machinery (PIM) components, and *3*) changes in mitochondrial membrane potential ($\Delta\Psi m$). Since p53 affects the underlying determinative indexes of protein import such as respiration and Ψm (22, 38, 54), we hypothesized that protein import would be altered in animals lacking p53. No prior studies exist that have examined the effect of p53 on protein import or on the expression of import machinery components in skeletal muscle.

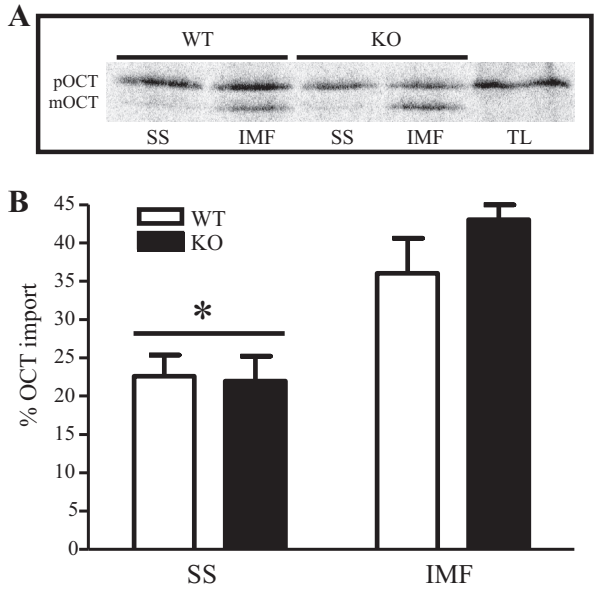

Fig. 5. Mitochondrial protein import of matrix-destined ornithine transcarbamylase (OCT) protein in SS and IMF mitochondria. Representative autoradiograms of protein import in the two mitochondrial populations from p53 WT and KO mice. *A*: quantification of protein import was determined as a ratio of mature OCT (mOCT) to total OCT [precursor OCT (pOCT) + mOCT]. *B*: TL, 5 μl of translation lane product that were not incubated with any mitochondria were run with each import reaction and used to verify translational efficiency. $^*P < 0.05$, SS vs. IMF mitochondrial subfraction; $n = 6–8$.

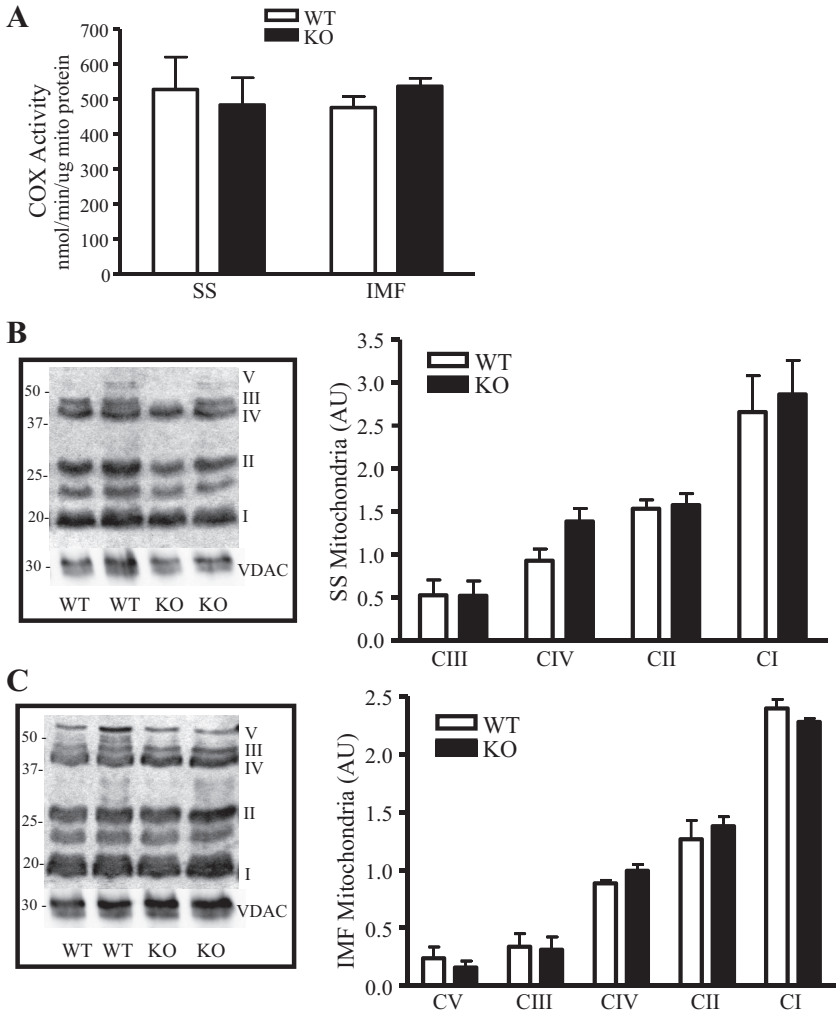

Fig. 6. Cytochrome *c* oxidase (COX) activity and expression of electron transport chain protein components in mitochondria from p53 WT and KO mice. COX activity was measured in isolated SS and IMF mitochondrial fractions from the 2 genotypes. *A*: values are expressed as means ± SE; $n = 8$. Representative Western blots (*left*) and the corresponding graphical representation (*right*) of components of ETC complexes in SS (*B*) and IMF (*C*) mitochondria from WT and KO samples. AU, arbitrary units. Values are expressed as means ± SE; $n = 4$.

Thus we investigated whether the levels of selected PIM components vital to the import of matrix-destined proteins were dependent on p53, and we related these findings to protein import kinetics into the organelle. Our analyses revealed protein- and mitochondrial fraction-specific decrements in key components of the import machinery, including Tom20, Tim23, mtHsp70, and mtHsp60, suggesting that p53 normally regulates the expression of these proteins. We subjected the upstream 2,000 bp of the mouse promoter regions of these PIM components to promoter analyses using Patch Software (http://www.gene-regulation.com/cgi-bin/pub/programs/patch/bin/patch.cgi). Bioinformatics revealed the presence of putative p53 response elements in the promoter regions of Tom20, Tim23, cpn10, and mtHsp60. Despite the fact that mtHSP70 was significantly reduced in the KO mitochondrial samples, no putative p53 binding sites were observed in the mtHsp70 promoter. Likewise, the cpn10 promoter possessed several p53 response motifs, yet its expression was not affected in the KO mice. This information reveals that the presence of consensus binding elements for p53 does not necessary determine the expression of its putative target gene and that other mechanisms, either direct or indirect, are likely involved in determining PIM component expression.

Alterations in the expression of PIM components, in conjunction with impaired respiration and membrane potential, would theoretically limit mitochondrial protein import. Thus we subsequently determined the mitochondrial import of a matrix-destined protein in isolated mitochondrial subfractions. As previously shown (46), IMF mitochondrial import was elevated compared with SS mitochondria, likely due to the higher respiration kinetics of the IMF mitochondrial pool. To our surprise, we observed no difference in the percent import of mOCT in either SS or IMF mitochondria between p53 WT and KO mice. Since mitochondrial preproteins also interact with cytosolic chaperones that mediate the unfolding and transport of newly synthesized proteins in intact cells in vivo, we also examined cytosolic chaperone expression. However, no changes were observed in the expression of Hsp90, Hsp70, and MSF-L, proteins that coordinate the localization of mitochondrial precursor proteins. Clearly, the mitochondrial capacity for protein import into the matrix is not impaired in the absence of p53 in skeletal muscle, despite a decrease in the expression of selected PIM components. Further research is warranted to examine the possibility that import into other submitochondrial localizations, such as the intermembrance space and inner/outer membranes, may be affected by the absence of p53.

Following the import process, subunits of holoenzymes must be assembled into functional ETC complexes. Using representative subunits located in each of complexes I, II, III, IV, and

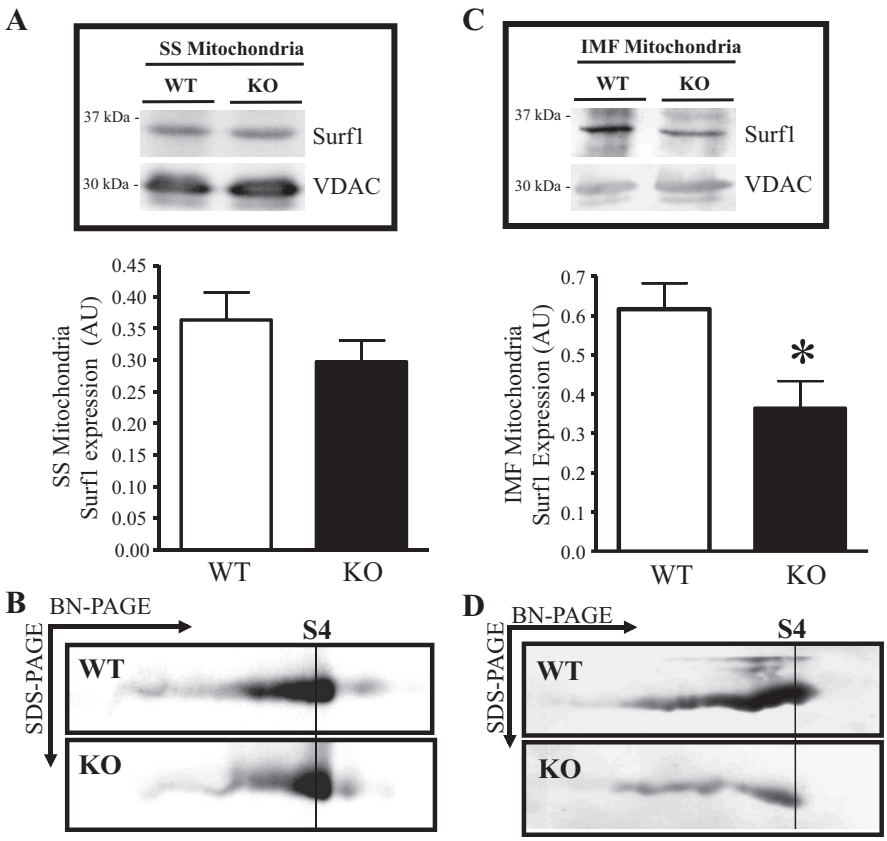

Fig. 7. Expression of Surf1 and mitochondrial COX assembly. Western blots along with graphical summaries depicting the expression of Surf1 in SS (*A*) and IMF (*C*) mitochondria. Values are expressed as means ± SE; $*P < 0.05$ vs. WT; $n = 5–7$. Blue native (BN)-PAGE gels were used to analyze the assembly of complex IV in SS (*B*) and IMF (*D*) mitochondria from WT vs. KO animals. S4 refers to the final assembly product and densitometric analysis revealed it to be deficient in the IMF mitochondria from KO mice ($*P < 0.05$; $n = 4$).

V, we noted no difference in their expression between the genotypes with respect to SS and IMF mitochondria. Furthermore, we had hypothesized that mitochondrial COX activity would be impaired in p53 KO mice due to previously reported defects in mitochondrial respiration (38), but our data revealed that COX activity was not different between the two genotypes in isolated SS or IMF mitochondria. The results of this experiment, although contrary to our expectations, are not necessarily contradictory to defective respiration rates, as mitochondrial oxidative phosphorylation is the culmination of the activity of the entire ETC, whereas COX activity reflects the function of complex IV in isolation from the other complexes. Moreover, this does not exclude the possibility of any changes in the activity of the native ETC complexes in the KO animals, which could be evaluated using complex-specific enzymatic assays or through BN-PAGE in gel activity techniques.

The COX complex is composed of 13 subunits, 2 copper centers, 2 hemes, and several cytochromes. The assembly of COX is thought to be a linear process that initiates around a seed formed by subunit I, subsequently assisted by a number of nuclear-encoded ancillary factors (45). The process involves four subcomplex assembly intermediate stages, and the final mature complex (S4) undergoes dimerization to result in the functional COX holoenzyme. To date, most disorders that involve COX deficiency are attributed to mutations in ancillary factors such as COX10 and COX15, which are important for heme A biosynthesis (2, 53); Surf1, which is essential for the formation of early assembly intermediates (59); and SCO1/2, which is required for COX copper metallation (16, 34, 52). Interestingly, despite documentation of p53-SCO2-dependent regulation of oxidative capacity in liver and cancer cell lines, SCO1/2 levels apparently do not decrease in the absence of p53 in skeletal muscle (35) and therefore may be relatively unimportant for the observed mitochondrial defect present in skeletal muscle of p53 KO animals. Thus we analyzed the expression of the assembly factor Surf1, which has been shown to be vital for the biogenesis of complex IV (59) and which contains a putative p53 response element in its promoter region (at nucleotide position −809) as revealed by in silico analysis done on the promoter region of the mus musculus Surf1 gene using the Patch Software. Our results show that Surf1 expression was significantly decreased in IMF mitochondria of KO animals. This decrement occurred in tandem with a decrease in the assembly of complex IV (S4) in the same mitochondrial pool. It is intriguing to speculate whether this delayed assembly process contributes to the oxidative defect present in mitochondria from p53 KO muscle (38), in spite of the unaffected complex IV activity and import kinetics.

Removal of p53 protein expression compromises not only the activity and content of mitochondria but also the architecture of these organelles, as we have previously shown (38). While p53 has been illustrated to affect mitochondrial dynamics and clearance, there is a dearth in literature with respect to its role in regulating these processes in skeletal muscle. Here we present a preliminary investigation into the effect of p53 on mitochondrial dynamics regulatory proteins, as well as autophagy-associated proteins, specifically related to the clearance of defective mitochondria under basal conditions.

For mitophagy to occur, dysfunctional organelles are segregated and processed into smaller, fragmented components to be

engulfed by autophagosomes (50). This fragmentation of mitochondria involves fission and fusion machinery components. The expression of p53 has previously been linked to mitochondrial morphology, such that the knockdown of p53 has been demonstrated to reduce mitochondrial fission when exposed to proapoptotic stimuli in cardiomyocytes (21); however, the effect of p53 on mitochondrial fusion and fission within skeletal muscle has not yet been addressed. Mitochondrial division involves the coordination of two regulatory proteins, Fis1 and Drp1 (11, 17), which appear to be differentially regulated by p53, based on our data. The expression of Drp1 is downregulated by the removal of p53, in corroboration with previous studies that found that p53 can transcriptionally regulate Drp1 (21, 55). Surprisingly, the absence of p53 also elicited an upregulation of Fis1 protein expression. This increase likely outweighs the reduction in Drp1 expression, since mitochondrial fragmentation was evident in p53 deficient muscle, a process that is thought to serve as a prerequisite for the onset of mitophagy (50). Future experiments will ascertain how p53 influences the processes of fission and fusion in real time using time-lapse microscopy and primary myotubes in cell culture.

With respect to autophagy, p53 null mice displayed an increase in ULK1 in cytosol from muscle, suggesting that p53 normally exerts a suppressive effect on its expression. Despite the higher ULK1 expression, the process of autophagy is likely attenuated in the p53 KO mice as evident from the accumulation of p62 in whole muscle fractions and lack of change in expression of other autophagy-related proteins such as LC3II, Beclin1, and ATG7 as we recently demonstrated (40). The decrease in cytosolic LC3II in the current article is likely a reflection of the translocation of LC3II from the cytosol to the mitochondrion. In addition, protein levels of lysosomal markers such as cathepsin D and lamp2 were also downregulated in the p53 KO muscle suggestive of impaired lysosomal activity (40). Mitochondrial p62 content was reduced in p53 KO mice, concomitant with elevated levels of LC3II localization to the organelle. This suggests that perhaps an increased drive for mitophagy persists in p53 KO mice, in accordance with recently published work by our laboratory (40). Furthermore, p53 ablation resulted in a reduction of both cytosolic and mitochondrial Parkin levels. While this may seem counterintuitive to the enhanced levels of promitophagic proteins measured in the KO mice, this supports the regulatory role of p53 in mediating Parkin expression, as demonstrated previously (58). We speculate that reduced Parkin levels may contribute to the irregular cristae organization and morphological deformities observed in the p53 KO mice, since Parkin-null mice have previously been shown to have abnormalities in their mitochondrial ultrastructure (9). Overall, our results demonstrate an increase in mitophagy-related protein expression, possibly to counteract the stress that occurs due to p53 ablation. However, although the upregulation of mitophagy may be important as an adaptive mechanism, it remains insufficient in magnitude, since an accumulation of damaged and irregular mitochondria persists in the absence of p53 as noted in this study. Indeed, subjecting p53 KO mice to a bout of acute exercise serves to increase the expression of both autophagy- and mitophagy-related protein markers indicating that exercise may play a therapeutic role in bringing the levels of autophagy/mitophagy back up to healthy control levels (40). While the changes in the protein content of these regulators of mitophagy are encouraging, further experiments that comprehensively measure mitophagy flux in the presence and absence of p53 will shed more light on this question.

In summary, while p53 plays an important role in determining oxidative capacity and mitochondrial function, the absence of this protein does not impair the vital processes involved in trafficking precursor proteins to the matrix components. More research is needed to elucidate the mechanisms underlying the decrease in several components of the import and assembly pathway, culminating in reduced COX assembly in the absence of p53. In addition, organelle morphology was affected by the ablation of p53, resulting in fragmented mitochondria. An upregulation in mitochondrial fission would allow for the segregation of dysfunctional mitochondria and subsequent removal by mitophagy. The specific role of p53 is important in this pathway, such that in its absence an upregulation of mitophagy appears to ensue.

ACKNOWLEDGMENTS

We thank Dr. Imogen Coe for use of the ultracentrifuge during the experiments and Leeann Bellamy for technical assistance provided during the study.

GRANTS

A. Saleem was funded by a Natural Sciences and Engineering Research Council (NSERC) Canada Graduate Scholarship and S. Iqbal was funded by a NSERC Postgraduate Scholarship. D. A. Hood holds a Canada Research Chair in Cell Physiology. This research was funded by an NSERC grant (to D. A. Hood).

DISCLOSURES

No conflicts of interest, financial or otherwise, are declared by the author(s).

AUTHOR CONTRIBUTIONS

Author contributions: A.S., S.I., and D.A.H. conception and design of research; A.S., S.I., and Y.Z. performed experiments; A.S. and S.I. analyzed data; A.S. and S.I. interpreted results of experiments; A.S. and S.I. prepared figures; A.S. and S.I. drafted manuscript; A.S., S.I., and D.A.H. edited and revised manuscript; A.S. and D.A.H. approved final version of manuscript.

REFERENCES

1. **Achanta G, Sasaki R, Feng L, Carew JS, Lu W, Pelicano H, Keating MJ, Huang P.** Novel role of p53 in maintaining mitochondrial genetic stability through interaction with DNA Pol gamma. *EMBO J* 24: 3482–3492, 2005.
2. **Antonicka H, Mattman A, Carlson CG, Glerum DM, Hoffbuhr KC, Leary SC, Kennaway NG, Shoubridge EA.** Mutations in COX15 produce a defect in the mitochondrial heme biosynthetic pathway, causing early-onset fatal hypertrophic cardiomyopathy. *Am J Hum Genet* 72: 101–114, 2003.
3. **Bjorkoy G, Lamark T, Brech A, Outzen H, Perander M, Overvatn A, Stenmark H, Johansen T.** p62/SQSTM1 forms protein aggregates degraded by autophagy and has a protective effect on huntingtin-induced cell death. *J Cell Biol* 171: 603–614, 2005.
4. **Bradford MM.** A rapid and sensitive method for the quantitation of microgram quantities of protein utilizing the principle of protein-dye binding. *Anal Biochem* 72: 248–254, 1976.
5. **Chacinska A, Koehler CM, Milenkovic D, Lithgow T, Pfanner N.** Importing mitochondrial proteins: machineries and mechanisms. *Cell* 138: 628–644, 2009.
6. **Chen H, Chomyn A, Chan DC.** Disruption of fusion results in mitochondrial heterogeneity and dysfunction. *J Biol Chem* 280: 26185–26192, 2005.
7. **Cogswell AM, Stevens RJ, Hood DA.** Properties of skeletal muscle mitochondria isolated from subsarcolemmal and intermyofibrillar regions. *Am J Physiol Cell Physiol* 264: C383–C389, 1993.
8. **Cooperstein SJ, Lazarow A.** A microspectrophotometric method for the determination of cytochrome oxidase. *J Biol Chem* 189: 665–670, 1951.

9. **Deng H, Dodson MW, Huang H, Guo M.** The Parkinson's disease genes pink1 and parkin promote mitochondrial fission and/or inhibit fusion in Drosophila. *Proc Natl Acad Sci USA* 105: 14503–14508, 2008.
10. **Donehower LA, Harvey M, Slagle BL, McArthur MJ, Montgomery CA Jr, Butel JS, Bradley A.** Mice deficient for p53 are developmentally normal but susceptible to spontaneous tumours. *Nature* 356: 215–221, 1992.
11. **Frank S, Gaume B, Bergmann-Leitner ES, Leitner WW, Robert EG, Catez F, Smith CL, Youle RJ.** The role of dynamin-related protein 1, a mediator of mitochondrial fission, in apoptosis. *Dev Cell* 1: 515–525, 2001.
12. **Gustafsson AB, Gottlieb RA.** Recycle or die: the role of autophagy in cardioprotection. *J Mol Cell Cardiol* 44: 654–661, 2008.
13. **Heath IB, Rethoret K.** Temporal analysis of the nuclear cycle by serial section electron microscopy of the fungus, Saprolegnia ferax. *Eur J Cell Biol* 21: 208–213, 1980.
14. **Hoogenraad NJ, Ward LA, Ryan MT.** Import and assembly of proteins into mitochondria of mammalian cells. *Biochim Biophys Acta* 1592: 97–105, 2002.
15. **Hoshino A, Mita Y, Okawa Y, Ariyoshi M, Iwai-Kanai E, Ueyama T, Ikeda K, Ogata T, Matoba S.** Cytosolic p53 inhibits Parkin-mediated mitophagy and promotes mitochondrial dysfunction in the mouse heart. *Nat Commun* 4: 2308, 2013.
16. **Jaksch M, Ogilvie I, Yao J, Kortenhaus G, Bresser HG, Gerbitz KD, Shoubridge EA.** Mutations in SCO2 are associated with a distinct form of hypertrophic cardiomyopathy and cytochrome c oxidase deficiency. *Hum Mol Genet* 9: 795–801, 2000.
17. **James DI, Parone PA, Mattenberger Y, Martinou JC.** hFis1, a novel component of the mammalian mitochondrial fission machinery. *J Biol Chem* 278: 36373–36379, 2003.
18. **Kabeya Y, Mizushima N, Ueno T, Yamamoto A, Kirisako T, Noda T, Kominami E, Ohsumi Y, Yoshimori T.** LC3, a mammalian homologue of yeast Apg8p, is localized in autophagosome membranes after processing. *EMBO J* 19: 5720–5728, 2000.
19. **Komatsu M, Waguri S, Koike M, Sou YS, Ueno T, Hara T, Mizushima N, Iwata J, Ezaki J, Murata S, Hamazaki J, Nishito Y, Iemura S, Natsume T, Yanagawa T, Uwayama J, Warabi E, Yoshida H, Ishii T, Kobayashi A, Yamamoto M, Yue Z, Uchiyama Y, Kominami E, Tanaka K.** Homeostatic levels of p62 control cytoplasmic inclusion body formation in autophagy-deficient mice. *Cell* 131: 1149–1163, 2007.
20. **Levine AJ.** p53, the cellular gatekeeper for growth and division. *Cell* 88: 323–331, 1997.
21. **Li J, Donath S, Li Y, Qin D, Prabhakar BS, Li P.** miR-30 regulates mitochondrial fission through targeting p53 and the dynamin-related protein-1 pathway. *PLoS Genet* 6: e1000795, 2010.
22. **Li PF, Dietz R, von Harsdorf R.** p53 regulates mitochondrial membrane potential through reactive oxygen species and induces cytochrome c-independent apoptosis blocked by Bcl-2. *EMBO J* 18: 6027–6036, 1999.
23. **Ljubicic V, Adhihetty PJ, Hood DA.** Role of UCP3 in state 4 respiration during contractile activity-induced mitochondrial biogenesis. *J Appl Physiol* 97: 976–983, 2004.
24. **Maddocks OD, Vousden KH.** Metabolic regulation by p53. *J Mol Med (Berl)* 89: 237–245, 2011.
25. **Matoba S, Kang JG, Patino WD, Wragg A, Boehm M, Gavrilova O, Hurley PJ, Bunz F, Hwang PM.** p53 regulates mitochondrial respiration. *Science* 312: 1650–1653, 2006.
26. **Meeusen S, DeVay R, Block J, Cassidy-Stone A, Wayson S, McCaffery JM, Nunnari J.** Mitochondrial inner-membrane fusion and crista maintenance requires the dynamin-related GTPase Mgm1. *Cell* 127: 383–395, 2006.
27. **Mihara K, Omura T.** Cytoplasmic chaperones in precursor targeting to mitochondria: the role of MSF and hsp 70. *Trends Cell Biol* 6: 104–108, 1996.
28. **Mihara K, Omura T.** Cytosolic factors in mitochondrial protein import. *Experientia* 52: 1063–1068, 1996.
29. **Morselli E, Tasdemir E, Maiuri MC, Galluzzi L, Kepp O, Criollo A, Vicencio JM, Soussi T, Kroemer G.** Mutant p53 protein localized in the cytoplasm inhibits autophagy. *Cell Cycle* 7: 3056–3061, 2008.
30. **Narendra D, Tanaka A, Suen DF, Youle RJ.** Parkin is recruited selectively to impaired mitochondria and promotes their autophagy. *J Cell Biol* 183: 795–803, 2008.
31. **Neupert W, Herrmann JM.** Translocation of proteins into mitochondria. *Annu Rev Biochem* 76: 723–749, 2007.
32. **Okatsu K, Saisho K, Shimanuki M, Nakada K, Shitara H, Sou YS, Kimura M, Sato S, Hattori N, Komatsu M, Tanaka K, Matsuda N.** p62/SQSTM1 cooperates with Parkin for perinuclear clustering of depolarized mitochondria. *Genes Cells* 15: 887–900, 2010.
33. **Pankiv S, Clausen TH, Lamark T, Brech A, Bruun JA, Outzen H, Overvatn A, Bjorkoy G, Johansen T.** p62/SQSTM1 binds directly to Atg8/LC3 to facilitate degradation of ubiquitinated protein aggregates by autophagy. *J Biol Chem* 282: 24131–24145, 2007.
34. **Papadopoulou LC, Sue CM, Davidson MM, Tanji K, Nishino I, Sadlock JE, Krishna S, Walker W, Selby J, Glerum DM, Coster RV, Lyon G, Scalais E, Lebel R, Kaplan P, Shanske S, De V, Bonilla E, Hirano M, DiMauro S, Schon EA.** Fatal infantile cardioencephalomyopathy with COX deficiency and mutations in SCO2, a COX assembly gene. *Nat Genet* 23: 333–337, 1999.
35. **Park JY, Wang PY, Matsumoto T, Sung HJ, Ma W, Choi JW, Anderson SA, Leary SC, Balaban RS, Kang JG, Hwang PM.** p53 improves aerobic exercise capacity and augments skeletal muscle mitochondrial DNA content. *Circ Res* 105: 705–12, 11, 2009.
36. **Priault M, Salin B, Schaeffer J, Vallette FM, di Rago JP, Martinou JC.** Impairing the bioenergetic status and the biogenesis of mitochondria triggers mitophagy in yeast. *Cell Death Differ* 12: 1613–1621, 2005.
37. **Saitoh T, Igura M, Obita T, Ose T, Kojima R, Maenaka K, Endo T, Kohda D.** Tom20 recognizes mitochondrial presequences through dynamic equilibrium among multiple bound states. *EMBO J* 26: 4777–4787, 2007.
38. **Saleem A, Adhihetty PJ, Hood DA.** Role of p53 in mitochondrial biogenesis and apoptosis in skeletal muscle. *Physiol Genomics* 37: 58–66, 2009.
39. **Saleem A, Carter HN, Iqbal S, Hood DA.** Role of p53 within the regulatory network controlling muscle mitochondrial biogenesis. *Exerc Sport Sci Rev* 39: 199–205, 2011.
40. **Saleem A, Carter HN, Hood DA.** p53 is necessary for the adaptive changes in cellular milieu subsequent to an acute bout of endurance exercise. *Am J Physiol Cell Physiol* 306: C241–C249, 2014.
41. **Schagger H, Cramer WA, von Jagow G.** Analysis of molecular masses and oligomeric states of protein complexes by blue native electrophoresis and isolation of membrane protein complexes by two-dimensional native electrophoresis. *Anal Biochem* 217: 220–230, 1994.
42. **Schagger H, von Jawow G.** Blue native electrophoresis for isolation of membrane protein complexes in enzymatically active form. *Anal Biochem* 199: 223–231, 1991.
43. **Scherz-Shouval R, Shvets E, Fass E, Shorer H, Gil L, Elazar Z.** Reactive oxygen species are essential for autophagy and specifically regulate the activity of Atg4. *EMBO J* 26: 1749–1760, 2007.
44. **Schmidt O, Pfanner N, Meisinger C.** Mitochondrial protein import: from proteomics to functional mechanisms. *Nat Rev Mol Cell Biol* 11: 655–667, 2010.
45. **Soto IC, Fontanesi F, Liu J, Barrientos A.** Biogenesis and assembly of eukaryotic cytochrome c oxidase catalytic core. *Biochim Biophys Acta* 1817: 883–897, 2012.
46. **Takahashi M, Hood DA.** Protein import into subsarcolemmal and intermyofibrillar skeletal muscle mitochondria. Differential import regulation in distinct subcellular regions. *J Biol Chem* 271: 27285–27291, 1996.
47. **Tanaka A, Cleland MM, Xu S, Narendra DP, Suen DF, Karbowski M, Youle RJ.** Proteasome and p97 mediate mitophagy and degradation of mitofusins induced by Parkin. *J Cell Biol* 191: 1367–1380, 2010.
48. **Tasdemir E, Chiara MM, Morselli E, Criollo A, D'Amelio M, Djavaheri-Mergny M, Cecconi F, Tavernarakis N, Kroemer G.** A dual role of p53 in the control of autophagy. *Autophagy* 4: 810–814, 2008.
49. **Tasdemir E, Maiuri MC, Galluzzi L, Vitale I, Djavaheri-Mergny M, D'Amelio M, Criollo A, Morselli E, Zhu C, Harper F, Nannmark U, Samara C, Pinton P, Vicencio JM, Carnuccio R, Moll UM, Madeo F, Paterlini-Brechot P, Rizzuto R, Szabadkai G, Pierron G, Blomgren K, Tavernarakis N, Codogno P, Cecconi F, Kroemer G.** Regulation of autophagy by cytoplasmic p53. *Nat Cell Biol* 10: 676–687, 2008.
50. **Twig G, Elorza A, Molina AJ, Mohamed H, Wikstrom JD, Walzer G, Stiles L, Haigh SE, Katz S, Las G, Alroy J, Wu M, Py BF, Yuan J, Deeney JT, Corkey BE, Shirihai OS.** Fission and selective fusion govern mitochondrial segregation and elimination by autophagy. *EMBO J* 27: 433–446, 2008.
51. **Uchiyama Y.** Autophagic cell death and its execution by lysosomal cathepsins. *Arch Histol Cytol* 64: 233–246, 2001.
52. **Valnot I, Osmond S, Gigarel N, Mehaye B, Amiel J, Cormier-Daire V, Munnich A, Bonnefont JP, Rustin P, Rotig A.** Mutations of the SCO1 gene

in mitochondrial cytochrome c oxidase deficiency with neonatal-onset hepatic failure and encephalopathy. *Am J Hum Genet* 67: 1104–1109, 2000.
53. **Valnot I, von Kleist-Retzow JC, Barrientos A, Gorbatyuk M, Taanman JW, Mehaye B, Rustin P, Tzagoloff A, Munnich A, Rotig A.** A mutation in the human heme A:farnesyltransferase gene (COX10) causes cytochrome c oxidase deficiency. *Hum Mol Genet* 9: 1245–1249, 2000.
54. **Wang F, Fu X, Chen X, Chen X, Zhao Y.** Mitochondrial uncoupling inhibits p53 mitochondrial translocation in TPA-challenged skin epidermal JB6 cells. *PLoS One* 5: e13459, 2010.
55. **Wang JX, Jiao JQ, Li Q, Long B, Wang K, Liu JP, Li YR, Li PF.** miR-499 regulates mitochondrial dynamics by targeting calcineurin and dynamin-related protein-1. *Nat Med* 17: 71–78, 2011.
56. **Yamamoto H, Esaki M, Kanamori T, Tamura Y, Nishikawa S, Endo T.** Tim50 is a subunit of the TIM23 complex that links protein translocation across the outer and inner mitochondrial membranes. *Cell* 111: 519–528, 2002.
57. **Young JC, Hoogenraad NJ, Hartl FU.** Molecular chaperones Hsp90 and Hsp70 deliver preproteins to the mitochondrial import receptor Tom70. *Cell* 112: 41–50, 2003.
58. **Zhang C, Lin M, Wu R, Wang X, Yang B, Levine AJ, Hu W, Feng Z.** Parkin, a p53 target gene, mediates the role of p53 in glucose metabolism and the Warburg effect. *Proc Natl Acad Sci USA* 108: 16259–16264, 2011.
59. **Zhu Z, Yao J, Johns T, Fu K, De B, I, Macmillan C, Cuthbert AP, Newbold RF, Wang J, Chevrette M, Brown GK, Brown RM, Shoubridge EA.** SURF1, encoding a factor involved in the biogenesis of cytochrome c oxidase, is mutated in Leigh syndrome. *Nat Genet* 20: 337–343, 1998.